Calculations of elastic electron scattering by H_2 for fixed nuclei

R. K. Nesbet

IBM Almaden Research Center, 650 Harry Road, San Jose, California 95120-6099

C. J. Noble

Science and Engineering Research Council, Daresbury Laboratory, Warrington WA4 4AD, England

L. A. Morgan

Department of Statistics and Computer Science, Royal Holloway College, Egham, Surrey TW20 OEX, England

Cross sections for elastic electron scattering by the $^1\Sigma_g^+$ ground state of H_2 are computed at fixed internuclear distance $1.402a_0$, for incident energies up to 13.6 eV. Variational R-matrix calculations are supplemented by asymptotic distorted-wave calculations for higher partial waves and by a residual Born-approximation sum for the polarization potential. Polarization response is treated dynamically, using $^1\Pi_u$ and $^1\Sigma_u^+$ polarization pseudostates obtained by variational calculations. Pseudostate closed channels are included in the coupled equations integrated outside an R-matrix sphere.

I. INTRODUCTION

Recent progress in experimental technique has made low-energy electron-molecule scattering a field of lively current interest. Experimental data, showing rich structure in the dependence of scattering cross sections on impact energy and on scattering angle, are often difficult to interpret. In the simpler case of electron-atom scattering, theoretical methodology has only recently been developed to the point where it can be used for quantitative predictions. The present work is concerned with the development of comparable capability for the quantitative theory of electron-molecule scattering.

A comprehensive review of the theory was published by Lane.[1] More recent developments are discussed by Buckley, Burke, and Noble.[2] Methods and results of accurate variational calculations of electron scattering by atoms have also been reviewed.[3] A particular strategy, combining aspects of R-matrix and matrix-variational methods, appears to be feasible for quantitative results. This strategy, which will be outlined here, is being pursued in a joint project among several research groups.

Burke and co-workers[4] have modified the ALCHEMY system of bound-state electronic wave function programs[5] for molecular R-matrix calculations. The variant of these programs developed by the present collaboration emphasizes polarization response of a target molecule and use of numerical asymptotic functions (NAF's) as basis functions in variational R-matrix calculations. Preliminary results[6] for the $^2\Sigma_u^+$ scattering state of $e^- + H_2$ were carried to effective basis-set convergence for energies up to 1.0 Ry, at fixed internuclear separation $1.402a_0$ (nuclear equilibrium in the $X\,^1\Sigma_g^+$ ground state). The present work extends these results, still at a fixed nuclear equilibrium, by considering all relevant aspects of convergence of the electronic wave function in all scattering states. This work is intended to provide a starting point for sub-

sequent quantitative studies of convergence and estimates of residual error, as was done in earlier benchmark calculations of $e^- + \text{He}$ scattering.[7]

With fixed nuclei, ignoring rovibrational motion, the principal theoretical problems in electron-molecule scattering are similar to those in electron-atom scattering, except that symmetry is reduced. In addition to the static screened-Coulomb potential of a neutral target molecule, scattering at low energies is strongly affected by long-range multipole potentials, which must be known accurately. The static dipole potential, if present, is dominant at low energies. For nonpolar molecular such as H_2, the static quadrupole and dipole polarization potentials are the most important. Experience with atoms[3] indicates that accurate results at low energies can only be obtained by a dynamical treatment of target polarization using dipole pseudostates or their equivalent. Despite recent progress in defining effective local potentials that simulate effects of electronic exchange and polarization,[8] definitive results require use of antisymmetric multichannel wave functions. The present methodology, described in Sec. II here, supports calculations of this general structure.

At the time of Lane's review article,[1] the most complete calculations of $e^- + H_2$ scattering were those of Klonover and Kaldor,[9] who computed a polarization optical potential to second order with respect to dipole transitions. This was used to obtain total and vibrational excitation cross sections in good agreement with experiment. More recently, Schneider and Collins[10] have incorporated a matrix optical potential in the linear-algebraic method. The Schwinger variational principle has been similarly modified by Gibson *et al.*,[11] incorporating polarization response as a multichannel closed-channel effect, and applied to $e^- + H_2$ scattering. Both of these calculations obtain total cross sections in good agreement with experiment and with the earlier calculations of Klonover and Kaldor.

Because of the difficulty of full multichannel electronic scattering calculations with conventional methods, most calculations of rovibrational excitation have simplified the electronic model by use of effective local potentials. Systematic calculations of this kind for $e^- + H_2$ have been carried out by Morrison and collaborators, with the goal of providing definitive results for comparison with experiment. The present situation for $e^- + H_2$ has been summarized recently by Crompton and Morrison.[12] Theory and experiment are in good agreement for the total cross section, as measured in beam experiments,[13-15] for energies up to 10 eV, and for the momentum-transfer cross section, as measured in electron-swarm experiments,[16] for energies up to 1.5 eV. Despite this agreement, there is a striking discrepancy for the $v = 0 \rightarrow v = 1$ vibrational excitation cross section between theory and experiment. One purpose of the present study is to provide a standard for comparison with model theory for fixed nuclei. At a later stage this work will be extended to include nuclear motion and to provide a standard for direct comparison with experiment.

The specific methodology used here is described in detail in Sec. II. This represents a continuation of a long line of prior developments. The variational R-matrix method, used here, treats electron exchange explicitly, through the use of antisymmetrized variational wave functions. Various approximate methods that model exchange scattering with a local potential are reviewed by Lane.[1] Direct integration of the integro-differential close-coupling equations with exchange can be carried out efficiently by reduction to linear-algebraic equations.[17] This method has been used for many calculations of electron scattering by atoms and atomic ions. More recent work by Schneider and Collins[10,18] extends this method to molecules, taking advantage of the great efficiency of parallel data processing.

Quantitative calculation of polarization effects in electron scattering involves a tradeoff between formal and computational difficulties.[1] Recent developments in local model polarization potentials include work by O'Connell and Lane[19] and by Padial and Norcross.[20] The linear-algebraic method has been extended to treat the nonlocal optical potential that describes dynamical effects of polarization in a pseudostate model.[10,18] In the present work, the system of coupled equations of the pseudostate model is integrated directly, including closed channels outside the R-matrix boundary. In accurate variational calculations of electron-atom scattering[3] these coupled equations were reduced to a matrix optical potential by an explicit matrix transformation. Accuracy of the pseudostates used in any such calculation can be judged from variational values of the polarization, and is comparable in all recent calculations on H_2. If all internal spin couplings are included in the coupled equations or in the equivalent matrix optical potential, accuracy is limited only by the completeness of the orbital basis set. Apparently both singlet and triplet virtual transitions to the polarization pseudostates were included in the work of Schneider and Collins.[10] There are, of course, many ways to achieve effective completeness of the orbital basis, including the use of off-center Gaussian orbitals.[18] The systematic procedure followed here is described in Sec. IV.

Another important line of development, followed here, is the use of Born or distorted-wave approximations to extend the partial-wave expansion to effective completeness. This is essential for polar target molecules,[21] since failure to take into account the rotational quenching of long-range static dipole scattering leads to false results. Frame-transformation theory has been used to treat this problem.[22] In the present work a multichannel distorted-wave method is used, as described below, to compute long-range effects of dipole polarization and of the static quadrupole potential for high partial waves.

Following a discussion of methodology in Sec. II, variational calculations of target-molecule ground-state and dipole pseudostates are described in Sec. III. Sections IV and V discuss basis-set and partial-wave convergence, respectively. Computed cross sections are presented in Sec. VI and compared with experiment and prior theory. Section VII is a summary and general discussion.

II. METHODOLOGY

Two distinct kinds of error occur in theoretical calculations: *structural* error due to inadequacy of the theoretical model, and *convergence* error due to simplification of calculations within this model. For meaningful estimates of residual errors, methods should be used that eliminate structural error, or at least reduce it below specified bounds, and that allow systematic study of convergence. It is essential that computer programs and computational algorithms be as free as possible from arbitrary constraints such as limits on basis-set size or on matrix dimensions. Variational methods are used by preference because they provide a formalism for successive improvement of accuracy.

In electron-molecule scattering, both target molecule and scattered electron must be represented to adequate accuracy, including their dynamical interaction. A great simplification occurs when the scattered electron is outside a radius r_1 sufficiently large that exchange with target electrons can be neglected. In this outer region, scattering is described by ordinary differential equations (close-coupling without exchange) containing asymptotic multipole potentials. Inside r_1, exchange must be taken into account, and the methodology must be adequate for a system of $N + 1$ electrons (assuming an N-electron target molecule). Bound-state variational methods are appropriate for the inner range of r. Alternative methods differ in their technique of matching solutions between the inner and outer ranges.

Quantitative results for electron-atom scattering were obtained with the R-matrix method[23] and with the matrix-variational method,[3] based on the Kohn-Hulthén variational principle. Recent studies[24] show that the main computational steps of these originally distinct methods can be made the same if numerical asymptotic functions (NAF's), obtained by solving the asymptotic close-coupling equations,[25,26] are used as variational basis functions.

In the present work, these ideas are implemented within the framework of variational R-matrix theory.[3,27,28] The

variational derivation places no condition on basis functions other than linear independence. The more traditional approach, using Green's theorem,[29] makes use of a complete set of basis functions in the interval $0 \leq r < r_1$, defined in practice by solving model equations with fixed boundary conditions at r_1.[23] The variational function of the standard theory has a discontinuity of slope at r_1. By removing this fixed boundary constraint, the variational R-matrix theory eliminates need for a Buttle correction[30] and can lead to more rapid basis-set convergence if basis functions are chosen appropriately.[24] Calculations differ from matrix-variational calculations primarily in that all integrals are truncated at the R-matrix boundary r_1, and the kinetic energy operator is symmetrized, equivalent to using a Bloch-modified Hamiltonian.[31]

Three distinct kinds of orbital basis functions are used in the present work, as described in a preliminary publication.[6] Atomic exponential basis functions [Slater-type orbitals (STO's)] are used for diatomic target states and pseudostates. At a later stage, Gaussian-type orbitals (GTO's) will be used for polyatomic molecules. Numerical asymptotic functions (NAF's) are included in the variational basis. These functions are computed by solving the asymptotic close-coupling equations between an inner matching radius r_0 and the R-matrix radius at r_1. The value of r_0 is chosen so that the target charge density lies primarily within r_0. Hence the close-coupling equations, with asymptotic multipole potentials, are approximately valid outside r_0, and completeness inside r_0 is assured by the atomic basis orbitals (STO's or GTO's). For the present calculation on H_2, r_0 is taken to be $2.0a_0$, while the R-matrix radius r_1 is set at $10.0a_0$, to ensure that exchange integrals are evaluated accurately with truncation at r_1. While the use of NAF's is found to provide rapid convergence at given scattering energy, these functions are energy dependent, as are the continuum basis functions of the matrix-variational method.[3] To avoid excessive computation of energy-dependent two-electron integrals, the smallest possible number of NAF's should be used. This is made possible by including energy-independent continuum basis functions in the form of regular spherical Bessel functions (RSB), or Coulomb functions for a molecular ion, with fixed boundary conditions at r_1. Calculations[6] on the $^2\Sigma_u$ scattering state of $e^- + H_2$, at nuclear equilibrium, showed that adequate convergence could be achieved with this mixed basis, over the energy range $k^2 = 0.01a_0^{-2}$ to $1.00a_0^{-2}$. To avoid linear dependence, only one NAF was used for each open channel, constructed as a linear combination of numerically integrated functions. The coefficients were determined by fitting to a diagonal R matrix (at r_0) defined by regular Bessel functions. Only the diagonal component of each multichannel NAF was used as a variational basis function.

The present work is the first to include pseudostate closed channels for a molecule in the coupled equations solved outside r_1. Traditional integration methods have difficulty with such strongly closed channels, because errors in wave functions grow exponentially in both directions of propagation. The method used here avoids propagation of wave functions. The variational R matrix at r_1 is propagated outwards[32,33] to an external radius r_G,

where it is matched to asymptotic multichannel wave functions obtained by an accelerated Gailitis method,[34] in which formal series expansions in powers of r^{-1} are converted to continued fractions.

To compute accurate differential cross sections, the partial-wave representation must be summed to convergence. The long-range multipole potentials typical of molecules can lead to significant contributions from partial waves of high order (large l values). Accurate variational calculations are feasible only for a few partial waves of low order. At any given energy, the partial-wave Born approximation is accurate for K-matrix elements at sufficiently large l. Such Born corrections are systematically included in the present work, as described in Sec. V, below.

The asymptotic distorted-wave method (ADW), which has been described elsewhere,[35] is used to bridge the gap between variational calculations for low l and direct use of the Born approximation for high l. This method was tested on preliminary calculations of the $^2\Sigma_u^+$ scattering state for $e^- + H_2$. Full solutions of the asymptotic close-coupling equations are matched at the inner radius r_0 onto a diagonal R matrix appropriate to regular Bessel functions, as in the definition of basis NAF's. In practice, the efficient integration technique used here outside r_1 is used to propagate the R matrix at r_0 out to r_G, where it is matched to a continued-fraction representation of the Gailitis expansion.[34]

Using these methods, the full dynamical structure due to specified target molecule states and polarization pseudostates is represented at all values of r. Basis-set convergence can be tested with alternative choices of orbital functions. The partial-wave series is approximated and summed rather than truncated.

III. WAVE FUNCTIONS OF THE TARGET MOLECULE

At this stage of the present project, target wave functions are required that have the simplest possible structure, while providing good approximate values of energy, quadrupole moment, and electric dipole polarizability. The programs used here[5] are designed for calculations with very elaborate variational wave functions, if needed for adequate convergence at a later stage.

All calculations reported here were carried out at internuclear distance $1.402a_0$ for H_2. In preliminary calculations on the $^2\Sigma_u^+$ scattering state,[6] the STO basis of Fraga and Ransil[36] for H_2, consisting of orbitals $1s\sigma$, $2s\sigma$, and $2p\sigma$ on each atom, was used. Six π orbitals were included, defined by multiplying the factor $x + iy$ into each σ orbital. For the $(1\sigma_g^2)^1\Sigma_g^+$ self-consistent-field (SCF) ground state, dipole pseudostates of the structure $(1\sigma_g \pi_u)^1\Pi_u$ and $(1\sigma_g \sigma_u)^1\Sigma_u^+$ were constructed from pseudoorbitals π_u and σ_u, respectively. The orbitals π_u and σ_u were defined by normalizing first-order dipole perturbation functions. Polarizabilities computed from these wave functions are

$$\alpha_{||} = 7.0149a_0^3, \quad \alpha_\perp = 4.9660a_0^3 . \tag{1}$$

These values are not sufficiently close to accurate values

TABLE I. STO orbital exponents.

$1s\sigma$	1.123,1.611
$2p\sigma$	1.123,1.611
$2p\pi,3p\pi$	1.084
$3d\pi$	2.470

of Kolos and Wolniewicz,[37]

$$\alpha_{||}=6.3805a_0^3, \quad \alpha_{\perp}=4.5777a_0^3 \ ,$$

at $r_{AB}=1.40a_0$, for use in the present scattering calculations.

An improved orbital basis was obtained using configuration-interaction (CI) representations of the $^1\Sigma_g^+$ target ground state and of $^1\Pi_u$ and $^1\Sigma_u^+$ dipole pseudostates. Calculations were organized similarly to earlier studies of atomic polarizabilities,[38] constructing pseudoorbitals to define virtual excitations in a CI expansion. Orbital exponents were chosen first to minimize $E_0(^1\Sigma_g^+)$, then varied to find local maxima of $\alpha_{||}$ and $\alpha_{\perp}$. An $(8\sigma,6\pi)$ STO basis was found to be needed for consistent results. Exponents for the final STO basis are listed in Table I.

In CI representation using all σ_g, σ_u, and π_u orbitals in this basis, there are 26 configuration-state functions of symmetry $^1\Sigma_g^+$, 12 of symmetry $^1\Pi_u$, and 16 of symmetry $^1\Sigma_u^+$. The computed CI ground-state energy is $-1.169\,894e^2/a_0$, with polarizabilities

$$\alpha_{||}=6.2654a_0^3, \quad \alpha_{\perp}=4.3590a_0^3 \ .$$

On introducing dipole pseudoorbitals π_u and σ_u, retaining only these orbitals and the SCF $1\sigma_g$ in the CI expansion, the ground-state manifold reduces to three configurations: $1\sigma_g^2$, π_u^2, and σ_u^2. The pseudostate manifolds $^1\Pi_u$ and $^1\Sigma_u^+$ reduce to single configurations, $1\sigma_g\pi_u$ and $1\sigma_g\sigma_u$, respectively. In this reduced CI representation, used for subsequent scattering calculations, the ground-state energy is $-1.141\,866e^2/a_0$ and the polarizabilities are

$$\alpha_{||}=6.2298a_0^3, \quad \alpha_{\perp}=4.4573a_0^3 \ .$$

The rotationally averaged dipole polarizability is $\alpha=5.0481a_0^3$, and the computed molecular quadrupole moment about the mass center is $Q=0.4470a_0^2$. For comparison, accurate values[37] are $\alpha=5.1786a_0^3$ and $Q=0.4575a_0^2$ at $r_{AB}=1.40a_0$.

As indicated by these numerical values, the present simple variational wave functions provide an approximation to the true molecular multipole moments that is adequate for scattering calculations within an error limit of several percent.

IV. BASIS-SET CONVERGENCE

Calculations were carried out for each of the six symmetry states listed in Table II, with orbital basis sets as shown. In each case, the fixed set of target STO's $(8\sigma,6\pi)$ defined in Table I was augmented by NAF and RSB continuum functions defined for $r \leq r_1$ about the scattering center (molecular-mass center). As described previously,[6]

convergence of the $^2\Sigma_u^+$ scattering state was studied by adding spherical Bessel functions to the NAF continuum basis $p\sigma_u, f\sigma_u$ until the eigenphase sum showed convergence to two or three significant decimals. Basis sets for the other symmetry states were derived from this $^2\Sigma_u^+$ basis by reassigning angular quantum numbers as required to represent polarization effects, but retaining the same number of RSB basis functions. In general, the RSB basis could be reduced by detailed study of convergence for each symmetry state.

The STO and RSB basis functions are independent of energy. The RSB basis for each scattering state is constructed by selecting, for each orbital angular symmetry indicated in Table II, radial functions with fixed boundary condition at r_1, in the order of increasing number of radial nodes. The spherical Bessel functions can be chosen either to have zero value at r_1 or to have zero slope. Both options were tested, and results were found to be insensitive to this choice of option. The zero-value option was used for results reported here.

In contrast to STO and RSB functions, the NAF basis functions and all integrals involving them are recomputed at each energy. Since NAF's are constructed as solutions of the asymptotic close-coupling equations without exchange, they are approximate solutions of the full radial scattering equations. Their use as basis functions in the open scattering channels leads to rapid convergence. Short-range effects are covered by the STO basis. Since the RSB basis is by itself a complete set for the open interval $0 \leq r < r_1$, residual effects of exchange, channel coupling, and short-range potentials are covered by including as many RSB functions as are necessary for convergence.

V. PARTIAL-WAVE CONVERGENCE

Although accurate variational calculations for molecules require major computational effort, consideration of the physics of low-energy electron scattering by small molecules indicates that such detailed calculations are necessary only for the lowest partial-wave states. A classical electron trajectory with angular momentum corresponding to quantum number l remains outside the turning radius r_{cl}, such that, in semiclassical approximation,

$$kr_{cl}=l+\tfrac{1}{2} \ . \tag{2}$$

In quantum mechanics, the corresponding partial-wave function is small inside r_{cl}. Hence, if r_{cl} exceeds the effective radius r_0 of a target molecule, electron scattering is only weakly influenced by the internal structure of the molecule. This fact is exploited in the ADW approximation,[35] in which only asymptotic multipole potentials are retained outside r_0.

For electron scattering by H_2, at impact energies up to 1.0 Ry ($k^2=1.0a_0^{-2}$), Eq. (2) implies that the ADW approximation should be valid for $l>\tfrac{3}{2}$. Hence, in all scattering states, only s and p partial waves can be strongly influenced by short-range interaction with the target molecule.

The present variational calculations used basis orbitals that represent partial waves with $l \leq 4$ in open channels associated with the $^1\Sigma_g^+$ electronic ground state of the tar-

TABLE II. Orbital basis sets.

State	Basis	s	σ_g d	g	σ_u p	f	π_u p	f	π_g d	g	δ_g d	g	δ_u f	Tot σ	Tot π	δ
$^2\Sigma_g^+$	STO		(4)		(4)		(3)		(3)					8	6	
	RSB	4	3		3	2	3	1	2					12	6	
	NAF	1	1	1										3		
														23	12	
$^2\Sigma_u^+$	STO		(4)		(4)		(3)		(3)					8	6	
	RSB	2	4	1	3	2	2	1	2	1				12	6	
	NAF				1		1							2		
														22	12	
$^2\Pi_u$	STO		(4)		(4)		(3)		(3)					8	6	
	RSB	4	3		3	2	2	1	2		2			12	5	2
	NAF						1	1							2	
														20	13	2
$^2\Pi_g$	STO		(4)		(4)		(3)		(3)					8	6	
	RSB	4	3		3	2	3	1	2					12	6	
	NAF								1	1					2	
														20	14	
$^2\Delta_g$	STO		(4)		(4)		(3)		(3)					8	6	
	RSB	4	3		3	2	3	1	2					12	6	
	NAF										1	1				2
														20	12	2
$^2\Delta_u$	STO		(4)		(4)		(3)		(3)					8	6	
	RSB	4	3		3	2	3	1	2					12	6	
	NAF												1			1
														20	12	1

get. These l values are well beyond the minimum indicated for validity of the ADW approximation. Using the continuum basis orbitals given in Table II, scattering states for the variational calculations were constructed with the channel structure indicated in rows var of Table III. Parameter N_{CF} is the number of configuration state functions in each variational calculation.

Recent calculations of e^-+H_2 scattering by Gibson et al.,[11] using a multichannel Schwinger method, showed that the triplet-coupled dipole pseudostates $(1\sigma_g\pi_u)^3\Pi_u$ and $(1\sigma_g\sigma_u)^3\Sigma_u^+$ make a substantial contribution to low-energy scattering. The present variational calculations include all configuration-state functions of given total symmetry obtained by coupling continuum basis orbitals to both singlet and triplet pseudostates. This structure, which allows for short-range exchange polarization, was implicit in earlier electron-atom scattering calculations based on variational solution of continuum Bethe-

Goldstone equations.[3] Because singlet-triplet transition dipole moments vanish, the triplet pseudostates do not produce long-range potentials in the asymptotic region.

ADW calculations[35] were carried out for the scattering states listed in Table III, with the channel structure indicated in rows ADW of the table. All open channels with $l \leq 7$ were included, together with all closed channels coupled to them by dipole-transition matrix elements. Parameter N_{ch} is the total number of coupled channels for each scattering state. Energies up to $k^2=1.0a_0^{-2}$ were considered.

If the axial angular momentum projection is Λ for the total scattering state and Λ_t for a target state, orbital quantum numbers $\lambda=\Lambda\pm\Lambda_t$ occur in degenerate scattering channels. In the present calculations, such channels are combined by a linear transformation that places all dipole-transition strength into a unique channel, decoupling the remaining degenerate pseudostate channels from

TABLE III. Scattering states and channel structure.

Scattering state			Target States		
			$^1\Sigma_g^+$	$^1\Pi_u$	$^1\Sigma_u^+$
$^2\Sigma_g^+$	$N_{ch}=12$		σ_g	π_u	σ_u
	ADW	$l=$	0,2,4,6	1,3,5,7	1,3,5,7
	var $N_{CF}=80$		0,2,4	1,3	1,3
$^2\Sigma_u^+$	$N_{ch}=13$		σ_u	π_g	σ_g
	ADW	$l=$	1,3,5,7	2,4,6,8	0,2,4,6,8
	var $N_{CF}=73$		1,3	2,4	0,2,4
$^2\Pi_u$	$N_{ch}=13$		π_u,δ_g	σ_g,δ_g	π_g
	ADW	$l=$	1,3,5,7	0,2,4,6,8	2,4,6,8
	var $N_{CF}=66$		1,3	0,2,4	2,4
$^2\Pi_g$	$N_{ch}=11$		π_g	σ_u,δ_u	π_u
	ADW	$l=$	2,4,6	1,3,5,7	1,3,5,7
	var $N_{CF}=63$		2,4	1,3	1,3
$^2\Delta_g$	$N_{ch}=10$		δ_g	π_u,ϕ_u	δ_u
	ADW	$l=$	2,4,6	1,3,5,7	3,5,7
	var $N_{CF}=19$		2,4	1,3	3
$^2\Delta_u$	$N_{ch}=10$		δ_u	π_g,ϕ_g	δ_g
	ADW	$l=$	3,5,7	2,4,6,8	4,6,8
	var $N_{CF}=19$		3	2,4	4

the ground state. These decoupled channels are omitted after transformation. Orbital quantum numbers λ are indicated in Table III for the transformed channel coupled to the $^1\Pi_u$ target pseudostate.

From the criteria given above, the ADW approximation should be accurate for $l > 3$, marginally valid for $l = 2$ or 3, but should fail for $l = 0$ or 1, in this energy range. Comparison with variational K-matrix elements, var in

Table IV, verifies this expected behavior. Final K matrices, for $l \leq 7$, were constructed by filling out the computed var K matrices with ADW elements. Thus, all the elements labeled var in Table IV were used, but the matrices were extended by inserting higher-order ADW elements. The degree of agreement found in the overlapping l ranges shown in Table IV indicates that this procedure is valid.

TABLE IV. Comparison of K-matrix elements, $k^2(a_0^{-1})$. The figure in brackets indicates a multiplying power of ten.

l_1	l_2	0.01 var	0.01 ADW	0.49 var	0.49 ADW	1.00 var	1.00 ADW
$^2\Sigma_g^+$							
0	0	-0.1741	0.1834	$-0.2976[+1]$	0.1082	$0.1699[+2]$	$0.3791[-1]$
2	0	$0.3637[-2]$	$0.3694[-2]$	$0.2130[-1]$	$0.1142[-1]$	0.4648	$-0.4327[-3]$
2	2	$0.3671[-2]$	$0.3712[-2]$	$0.8621[-1]$	$0.7330[-1]$	0.1349	0.1199
4	0	$-0.3411[-8]$	$0.1273[-6]$	$-0.1804[-4]$	$0.1089[-4]$	$-0.9903[-3]$	$0.6602[-4]$
4	2	$0.4979[-3]$	$0.4981[-3]$	$0.4802[-2]$	$0.4121[-2]$	$0.1152[-1]$	$0.5679[-2]$
4	4		$0.8225[-3]$		$0.1528[-1]$		$0.2904[-1]$
$^2\Sigma_u^+$							
1	1	$0.2305[-1]$	$0.1912[-1]$	$0.1295[+1]$	0.1884	$0.1257[+1]$	0.1830
3	1	$0.1040[-2]$	$0.1040[-2]$	$0.1851[-1]$	$0.7429[-2]$	$0.2907[-1]$	$0.7306[-2]$
3	3	$0.1524[-2]$	$0.1525[-2]$	$0.2972[-1]$	$0.3054[-1]$	$0.4895[-1]$	$0.5772[-1]$
$^2\Pi_u$							
1	1	$0.4046[-2]$	$0.3962[-2]$	0.3326	0.1013	0.4826	$0.9863[-1]$
3	1	$0.8006[-3]$	$0.7941[-3]$	$0.1235[-1]$	$0.4910[-2]$	$0.1828[-1]$	$0.5667[-2]$
3	3	$0.1268[-2]$	$0.1270[-2]$	$0.1896[-1]$	$0.2828[-1]$	$0.4232[-1]$	$0.5298[-1]$

In the variational calculations for scattering states $^2\Sigma_g^+$, $^2\Pi_g$, and $^2\Delta_g$, channel orbitals with $l=4$ were included in the calculations, but closed-channel orbitals with $l=5$ were omitted, as indicated in Table III. This omits dipole-transition elements and systematically underestimates the corresponding diagonal K-matrix elements,[35] as was checked in trial calculations. In these cases the 4,4 elements of the var K matrices were replaced by the corresponding ADW element, as indicated in Table IV for the $^2\Sigma_g^+$ state. Lower-order var elements were retained. Trial calculations at $k^2=0.01a_0^{-2}$ verified that these elements are not significantly changed by including $l=5$ closed channels in the coupled equations.

Dynamical effects of channel coupling can be represented by an optical potential in each open scattering channel. An asymptotic expansion of this optical potential in powers of r^{-1} has been derived[39] by analyzing the Gailitis expansion[40] of solutions of the asymptotic close-coupling equations. Because wave functions are small inside the classical centrifugal barrier, for sufficiently large partial-wave l values scattering effects are dominated by the leading terms in this asymptotic expansion of the optical potential. At any given energy, the partial-wave Born approximation becomes valid at sufficiently large l, and can be applied to the leading terms of the optical potential in each open channel. This method is used in the present work to complete the partial-wave expansion beyond the range of l values considered in ADW calculations.

For a neutral nonpolar molecule, the two leading terms of the optical potential in a channel with orbital quantum numbers l,m (quantized with reference to the molecular axis) are

$$2V_{lm}(r)=-2Q_{lm}/r^3-\alpha_{lm}/r^4 . \tag{3}$$

The constants here are an effective quadrupole moment

$$2Q_{lm}=-a^{(2)}_{lm,lm} \tag{4}$$

and an effective polarizability

$$\alpha_{lm}=\sum_{l',m'}(a^{(1)}_{lm,l'm'})^2/2\Delta E , \tag{5}$$

defined in terms of the asymptotic multipole potential coefficients $a^{(s)}$ derived by Burke et al.,[4] and of the pseudostate excitation energies ΔE, in hartree units. The coefficients in Eq. (3) satisfy the sum rules

$$\sum_m Q_{lm}=0$$

and

$$\frac{1}{2l+1}\sum_m \alpha_{lm}=\alpha , \tag{6}$$

where α is the spherically averaged molecular polarizability.

The partial-wave Born formulas for approximate K-matrix elements (tanδ, where δ is a phase shift) are,[3] for $l>0$,

$$\tan\delta_{Qlm}=2Q_{lm}k\int_0^\infty z^{-1}j_l^2(z)dz=\frac{Q_{lm}k}{l(l+1)} ,$$

$$\tan\delta_{\alpha lm}=\alpha_{lm}k^2\int_0^\infty z^{-2}j_l^2(z)dz \tag{7}$$

$$=\frac{\pi\alpha_{lm}k^2}{(2l-1)(2l+1)(2l+3)} .$$

The resulting first Born partial cross section is

$$\Delta\sigma_{lm}^{(B1)}=\frac{4\pi}{k^2}\sin^2(\delta_{Qlm}+\delta_{\alpha lm}) . \tag{8}$$

This formula was used to evaluate partial cross sections for $3\leq l\leq 7, 3\leq|m|$. Examples of this formula are given in Table V for $|m|=2$, corresponding to scattering states $^2\Delta_g$ and $^2\Delta_u$. In this table, $B_{\rm sum}$ is the sum of $\Delta\sigma_{lm}^{(B1)}$ over open-channel l values for the indicated scattering state (with $l\leq7$), while $Q_{\rm sum}$ is the partial cross section computed by combining var and ADW K matrices as described above. The $Q_{\rm sum}$ values shown in Table V, assumed to be accurate, are added into the cross sections reported here. The $B_{\rm sum}$ terms, evaluated for $|m|=2$, are shown only for comparison. $B_{\rm sum}$ terms were included in final results only for $|m|\geq3$, beyond the range of detailed K-matrix calculations in this work.

The first Born approximation should be valid in general when the scattered-wave amplitude is small, hence when a partial-wave cross section is small. The truncated optical potential of Eq. (3) must be valid at specified energy for sufficiently large l. A more specific criterion has not been derived. The data shown in Table V indicate that both Born approximation and optical potential are valid for $k^2=0.01a_0^{-2}, l\geq2$. The combined approximation loses accuracy as energy increases. Of the $B_{\rm sum}$ terms that are retained here (with $|m|\geq3$), even at $k^2=1.00a_0^{-2}$ the largest single term is 0.1449×10^{-1}. The sum of these terms is 0.5665×10^{-1}, compared with total cross section 7.2384, in units 10^{-16} cm^2. Hence any residual error in the Born sum is negligible here.

The partial-wave Born terms can be summed to infinite

TABLE V. Comparison of partial cross sections (10^{-16} cm^2), $k^2(a_0^{-2})$. The figure in brackets indicates a multiplying power of ten.

State	0.01		0.49		1.00	
	$Q_{\rm sum}$	$B_{\rm sum}$	$Q_{\rm sum}$	$B_{\rm sum}$	$Q_{\rm sum}$	$B_{\rm sum}$
$^2\Delta_g$	0.2842[−2]	0.2032[−2]	0.3427[−1]	0.1599	0.1454	0.3716
$^2\Delta_u$	0.1179[−2]	0.1067[−2]	0.9931[−2]	0.3502[−1]	0.1913[−1]	0.7034[−1]

order in closed form.[3,41] This should be done when computing differential cross sections, in order to describe forward-scattering structure. In the present case, since Q_{lm} sums to zero (spherical averaging), only the polarizability term is considered. The residual Born sum of partial cross sections with $l \geq l_B$ for the spherically averaged polarizability α is

$$\Delta\sigma_\alpha^{(B1)}(l_B) = \tfrac{1}{2}\pi^3\alpha^2 k^2 S(l_B) , \qquad (9)$$

where

$$S(l_B) = \sum_{l=l_B}^{\infty} \frac{8}{(2l-1)^2(2l+1)(2l+3)^2} . \qquad (10)$$

It can easily be verified, from the difference between successive sums, that

$$S(l_B) = \frac{1}{(4l_B^2-1)^2} . \qquad (11)$$

Hence Eq. (9) reduces to

$$\Delta\sigma_\alpha^{(B1)}(l_B) = \tfrac{1}{2}\pi^3\alpha^2 k^2/(4l_B^2-1)^2 . \qquad (12)$$

With $l_B = 8$ and $k^2 = 1.00a_0^{-2}$, this residual sum is 0.6076×10^{-2}, compared with total cross section 7.2187, in units 10^{-16} cm^2. This sum is included in final results reported here, although it is negligible to the present level of accuracy.

VI. CROSS SECTIONS

Table VI lists cross sections computed as described in Secs. IV and V at fixed internuclear distance $r_{AB} = 1.402a_0$, for energies up to 1.0 Ry ($k^2 = 1.00a_0^{-2}$). Partial elastic cross sections in symmetry states $^2\Sigma_g^+$, $^2\Sigma_u^+$, and $^2\Pi_u$ are shown in Figs. 1, 2, and 3. Comparison is made with data from a recent publication by Gibson, Lima, Takatsuka, and McKoy.[11] These authors compared full SEP (static-exchange plus polarization) results, computed by a multichannel Schwinger method, with SEPS (restricted to singlet polarization states) and SE (static ex-

change) calculations, all shown in the Figures. Also shown are SEP calculations of Gibson and Morrison[8] (GM), who used a nonempirical dipole polarization potential, and of Schneider and Collins[10] (SC), who used a separable expansion of the nonlocal optical potential due to target polarization. These recent calculations are expected to be more accurate than the earlier second-order optical-potential calculation of Klonover and Kaldor,[9] not included in the present figures. Labels for all curves in Figs. 1–3 are shown in Fig. 1.

Figure 1 shows the partial integral cross section in scattering state $^2\Sigma_g^+$. The general trend is that the static-exchange cross section is progressively reduced by more complete inclusion of polarization. The SEPS and SEP calculations of Gibson et al.,[11] follow this trend. The present results, which are designed to be close to convergence, continue this trend. If analogous to $e^- + $He s-wave scattering,[3] the $^2\Sigma_g^+$ cross section should rise from a finite value at zero energy to a low-energy peak, then fall gradually with increasing energy, in agreement with the present calculations. Resonances of this symmetry are not expected below 10 eV, since the first excited electronic state (the $b\,^3\Sigma_u^+$ repulsive state) occurs at that energy for $r_{AB} = 1.402a_0$. Although the calculations of Schneider and Collins[10] and of Gibson and Morrison[8] nearly coincide, they differ from the present results by more than the expected present error. Systematic investigation of residual errors is required before a definite conclusion can be drawn from this comparison.

Figure 2 shows the computed cross section in scattering state $^2\Sigma_u^+$. The broad peak near 4 eV is influenced by the well-known shape resonance, whose width is large at $r_{AB} = 1.402a_0$. For energies below 10 eV, the present results agree closely with the full SEP calculations of Gibson et al.[11] Preliminary calculations, reported previously,[6] omitted triplet pseudostates as did the SEPS data of Gibson et al.[11] These results are in good agreement. As in the results for $^2\Sigma_g^+$ symmetry, there is substantial disagreement between the present results and those of Refs. 8 and 10, outside the present expected error.

At the largest energies considered here, a narrow Feshbach resonance is found in the $^2\Sigma_u^+$ scattering state. Wave-function structure corresponds to a σ_g electron attached to the $B(^1\Sigma_u^+)$ electronic excited state. Detailed

TABLE VI. Computed partial cross sections, $\sigma(10^{-16}$ cm$^2)$.

k^2	E (eV)	$^2\Sigma_g^+$	$^2\Sigma_u^+$	$^2\Pi_u$	$^2\Pi_g$	$^2\Delta_g$	$^2\Delta_u$	Total[a]
0.01	0.14	10.370	0.189	0.020	0.005	0.001	0.000	10.586
0.04	0.54	11.288	0.742	0.163	0.010	0.001	0.001	12.205
0.09	1.22	11.121	1.859	0.519	0.014	0.001	0.001	13.515
0.16	2.18	10.186	3.514	1.029	0.021	0.001	0.001	14.755
0.25	3.40	9.051	4.635	1.414	0.036	0.003	0.001	15.142
0.36	4.90	7.824	4.857	1.597	0.051	0.006	0.002	14.341
0.49	6.67	6.508	4.507	1.613	0.061	0.010	0.003	12.708
0.64	8.71	5.381	3.909	1.527	0.079	0.015	0.003	10.925
0.81	11.02	4.429	3.464	1.403	0.084	0.023	0.004	9.419
1.00	13.61	3.563	2.166	1.367	0.079	0.041	0.005	7.238

[a]Includes Born increment. See Sec. V of text.
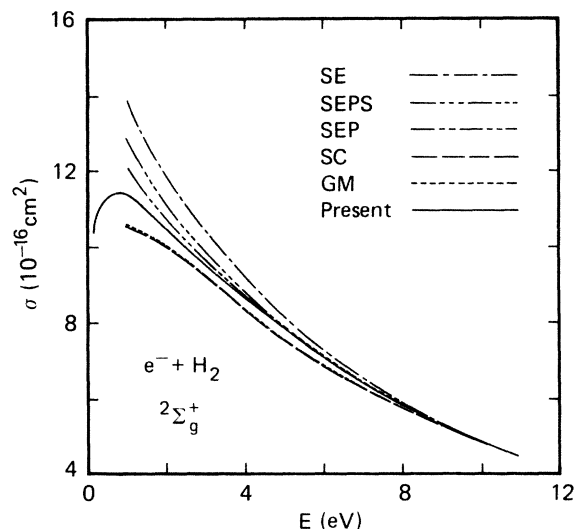
FIG. 1. $e^- + H_2$ elastic cross section, $^2\Sigma_g^+$ symmetry.
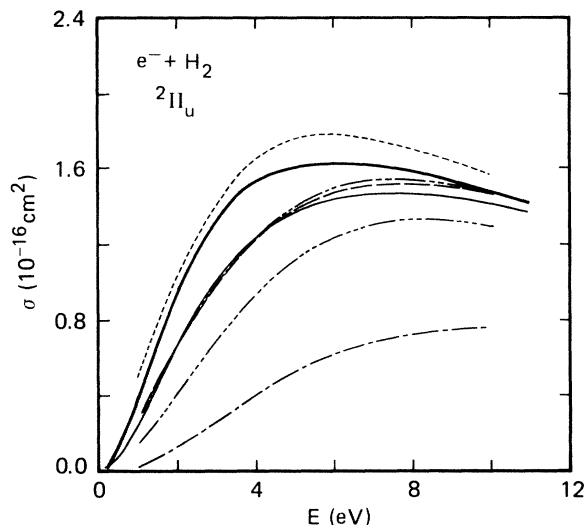
FIG. 3. $e^- + H_2$ elastic cross section, $^2\Pi_u$ symmetry.

variational calculations of this resonance will be reported elsewhere. The local upward trend of the $^2\Sigma_u^+$ cross section above 10 eV, shown in Fig. 3, is due to this resonance.

Figure 3 shows the computed cross section in scattering state $^2\Pi_u$. The wider full curve represents the present final data. The narrower full curve shows calculations omitting RSB basis orbitals of $d\delta_g$ symmetry, which are needed for full representation of the polarization effect inside r_1. The present results are consistent with the trend with increasingly complete treatment of polarization in the calculations of Gibson et al.[11] Calculations without $d\delta_g$ basis orbitals are close to their SEP results. When $d\delta_g$ orbitals are included, the present results are closer to the calculations of Gibson and Morrison,[8] indicating that the latter work more effectively models the polarization potential in this case. The results of Schneider and Col-

lins[10] nearly coincide with the SEP calculation of Gibson et al.[11]

As described in Sec. V, final K matrices were constructed here by combining data from variational and ADW calculations. Eigenphase sums computed from these K matrices are listed in Table VII. Open channel indices for each scattering state are defined by entries for the $^1\Sigma_g^+$ target ground state, in Table III. The $^2\Sigma_u^+$ eigenphase sum increases through π radians at a Feshbach resonance between $k^2 = 0.81a_0^2$ and $1.00a_0^2$. Because the parent state $B\,^1\Sigma_u^+$ has not been computed directly in the present work, the resonance energy is not well determined here. Other narrow resonances associated with excited electronic states may occur below 13.61 eV, but no systematic search has been carried out for them.

The total elastic cross section computed at $r_{AB} = 1.402a_0$ is shown in Fig. 4. The present results in-
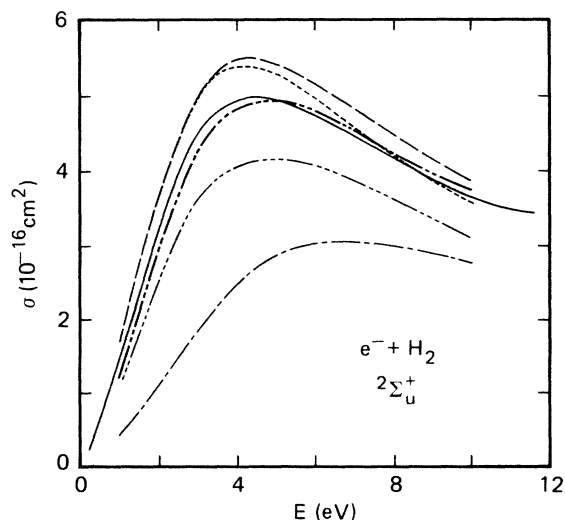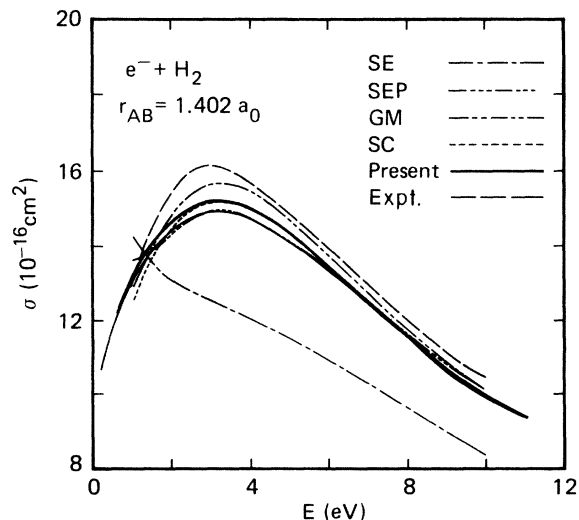

FIG. 2. $e^- + H_2$ elastic cross section, $^2\Sigma_u^+$ symmetry.

FIG. 4. $e^- + H_2$ total cross sections.

TABLE VII. Eigenphase sums.

k^2	E (eV)	$^2\Sigma_g^+$	$^2\Sigma_u^+$	$^2\Pi_u$	$^2\Pi_g$	$^2\Delta_g$	$^2\Delta_u$
0.01	0.14	2.9740	0.0253	0.0070	0.0036	0.0000	0.0009
0.04	0.54	2.7882	0.0977	0.0353	0.0100	0.0020	0.0030
0.09	1.22	2.6025	0.2299	0.0903	0.0176	0.0041	0.0055
0.16	2.18	2.4324	0.4262	0.1657	0.0288	0.0078	0.0076
0.25	3.40	2.2735	0.6329	0.2421	0.0457	0.0156	0.0099
0.36	4.90	2.1228	0.8136	0.3124	0.0646	0.0274	0.0140
0.49	6.67	2.0020	0.9555	0.3725	0.0828	0.0394	0.0220
0.64	8.71	1.8928	1.0520	0.4214	0.1075	0.0550	0.0261
0.81	11.02	1.8118	1.1606	0.4633	0.1265	0.0742	0.0337
1.00	13.61	1.6730	4.1126	0.5195	0.1394	0.1051	0.0434

clude corrections for high-order partial waves, as described in Sec. V, and are expected to be accurate to within several percent. The wide and narrow full curves in Fig. 4 correspond to the two different $^2\Pi_u$ calculations shown in Fig. 3. The present final results (upper solid curve) agree closely with Schneider and Collins (SC),[10] while the lower curve, omitting $d\delta_g$ basis orbitals in computing the $^2\Pi_u$ partial cross section, agrees closely with the full SEP calculation of Gibson et al.[11] The experimental data of Jones,[15] shown in the figure, are for the total cross section, including vibrational excitation. Preliminary results of vibrational averaging, extending the present calculations over a range of internuclear distances, indicate an increase in the total cross section large enough to account for the difference between experiment and fixed-nuclei theory indicated in Fig. 4. The calculations of Gibson and Morrison (GM) (Ref. 8) lie well above the present data. Since there was no vibrational averaging, the indicated better agreement with experiment appears to be fortuitous. Inadequacy of the static-exchange approximation (SE) (Ref. 11) is evident from the data given.

VII. DISCUSSION

The goal of the present project is to obtain theoretical electron-molecule scattering cross sections of quantitative accuracy. Such results are needed to calibrate experiment as well as to provide a benchmark test for approximate theoretical methods. In prior theoretical calculations of $e^- + $He scattering,[7] error limits of 1% have been achieved for the differential elastic cross section at all scattering angles, for energies up to 19 eV.

The present project has assembled the computational capability required for calculations of comparable high accuracy at fixed nuclear geometry, for diatomic target molecules. Calculations of the same kind as those reported here are capable of reducing the residual error below the present several percent, primarily by increasing the orbital-basis set in calculating target states and scattering wave functions. The computed results presented here provide a starting point, already at a good level of accuracy and internal consistency, for systematic study and reduction of residual errors.

For comparison with experiment, the theoretical treatment of rovibrational motion must be carried out at a similarly high level of accuracy. Several alternative methods are available, and will be tested in the next stage of this project.

[1]N. F. Lane, Rev. Mod. Phys. 52, 29 (1980).
[2]B. D. Buckley, P. G. Burke, and C. J. Noble, in Electron-Molecule Collisions, edited by I. Shimamura and K. Takayanagi (Plenum, New York, 1982).
[3]R. K. Nesbet, Variational Methods in Electron-Atom Scattering Theory (Plenum, New York, 1980).
[4]P. G. Burke, I. Mackey, and I. Shimamura, J. Phys. B 10, 2497 (1977); J. Kendrick and B. D. Buckley, Daresbury Laboratory Internal Report, DL/SCI/TM22T, 1980 (unpublished); C. J. Noble, Daresbury Laboratory Internal Report, DL/SCI/TM33T, 1982 (unpublished).
[5]A. D. McLean, M. Yoshimine, P. Bagus, and B. Liu, ALCHEMY programs, IBM San Jose Research Laboratory, as described

by A. D. McLean in Proceedings of the Conference on Potential Energy Surfaces in Chemistry, IBM Research Laboratory, San Jose, 1971, edited by W. A. Lester, Jr. (unpublished).
[6]R. K. Nesbet, C. J. Noble, L. A. Morgan, and C. A. Weatherford, J. Phys. B 17, L891 (1984).
[7]R. K. Nesbet, Phys. Rev. A 20, 58 (1979); J. Phys. B 12, L243 (1979).
[8]T. L. Gibson and M. A. Morrison, Phys. Rev. A 29, 2497 (1984).
[9]A. Klonover and U. Kaldor, J. Phys. B 12, 323 (1979); 12, 3797 (1979).
[10]B. I. Schneider and L. A. Collins, J. Phys. B 15, L335 (1982); Phys. Rev. A 27, 2847 (1983).

[11]T. L. Gibson, M. A. P. Lima, K. Takatsuka, and V. McKoy, Phys. Rev. A 30, 3005 (1984).

[12]R. W. Crompton and M. A. Morrison, in *Swarm Studies of Inelastic Electron-Molecule Collisions,* edited by L. C. Pitchford and V. McKoy (Springer-Verlag, New York, 1985).

[13]J. Ferch, W. Raith, and K. Schroder, J. Phys. B 13, 1481 (1980).

[14]G. Dalba, P. Fornasini, I. Lazzizzera, G. Ramieri, and A. Zecca. J. Phys. B 13, 2898 (1980).

[15]R. K. Jones, Phys. Rev. A 31, 2898 (1985).

[16]R. W. Crompton, D. K. Gibson, and A. I. McIntosh, Australian J. Phys. 22, 715 (1969); R. W. Crompton, D. K. Gibson, and A. G. Robertson, Phys. Rev. A 2, 1386 (1970).

[17]W. Eissner and M. J. Seaton, J. Phys. B 5, 2187 (1972); M. J. Seaton, *ibid.* 7, 1817 (1974).

[18]B. I. Schneider and L. A. Collins, Phys. Rev. A 30, 95 (1984); L. A. Collins And B. I. Schneider, J. Phys. B 17, L235 (1984).

[19]J. K. O'Connell and N. J. Lane, Phys. Rev. A 27, 1893 (1983).

[20]N. T. Padial and D. W. Norcross, Phys. Rev. A 29, 1742 (1984).

[21]D. W. Norcross and L. A. Collins, Adv. At. Mol. Phys. 18, 341 (1982).

[22]J. Siegel, J. L. Dehmer, and D. Dill, Phys. Rev. A 23, 632 (1981).

[23]P. G. Burke and W. D. Robb, Adv. At. Mol. Phys. 11, 143 (1975).

[24]R. K. Nesbet, Phys. Rev. A 24, 2975 (1981); J. Phys. B 14, L415 (1981).

[25]R. S. Oberoi and R. K. Nesbet, J. Comput. Phys. 12, 526 (1973).

[26]L. A. Morgan, J. Phys. B 13, 3703 (1980).

[27]J. L. Jackson, Phys. Rev. 83, 301 (1951).

[28]R. S. Oberoi and R. K. Nesbet, Phys. Rev. A 8, 215 (1973); 9, 2804 (1974).

[29]E. P. Wigner and L. Eisenbud, Phys. Rev. 72, 29 (1947); A. M. Lane and R. G. Thomas, Rev. Mod. Phys. 30, 257 (1958).

[30]P. J. A. Buttle, Phys. Rev. 160, 719 (1967).

[31]C. Bloch, Nucl. Phys. 4, 503 (1970).

[32]K. L. Baluja, P. G. Burke, and L. A. Morgan, Comput. Phys. Commun. 27, 299 (1982).

[33]J. C. Light and R. B. Walker, J. Chem. Phys. 64, 4272 (1976).

[34]C. J. Noble and R. K. Nesbet, Comput. Phys. Commun. 33, 399 (1984).

[35]R. K. Nesbet, J. Phys. B 17, L897 (1984).

[36]S. Fraga and B. J. Ransil, J. Chem. Phys. 35, 1967 (1961).

[37]W. Kolos and L. Wolniewicz, J. Chem. Phys. 46, 1426 (1967).

[38]R. K. Nesbet, Phys. Rev. A 16, 1 (1977).

[39]R. K. Nesbet, Abstracts of the Fifth West Coast Theoretical Chemistry Conference, SRI Menlo Park, California, 1983 (unpublished).

[40]M. Gailitis, J. Phys. B 9, 843 (1976).

[41]D. G. Thompson, Proc. R Soc. London A 294, 160 (1966).